Dependence of the apex angle of an inverted pyramidal-shaped container on crystallization of Brownian particles

Dependence of the Apex Angle of an Inverted Pyramidal-Shaped Container on Crystallization of Brownian Particles

Youhei Kanatsu[1] and Masahide Sato[2] [*]

[1] *Graduate School of Natural Science and Technology, Kanazawa University, Kakuma, Kanazawa 920-1192, Japan*

[2] *Information Media Center, Kanazawa University, Kakuma, Kanazawa 920-1192, Japan*

Large grains of a close-packed colloidal crystal have been experimentally shown to form in an inverted pyramidal pit by sedimentation [S. Matsuo, T. Fujine, K. Fukuda, S. Juodkazis, and H. Misawa, Appl. Phys. Lett. **82**, 4285 (2003)]. Keeping this experiment in mind, we study the crystallization of Brownian particles. We carry out Brownian dynamics simulations in an inverted pyramidal-shaped container. The Brownian particles settle out toward the apex of the container by a uniform external force. If the apex angle is suitable, large grains with the face-centered cubic (fcc) structure are formed [Y. Kanatsu and M. Sato, J. Phys. Soc. Jpn. **84**, 044601 (2015)]. When the apex angle deviates from a suitable value, the number of hexagonal close-packed (hcp) structured particles, N_{hcp}, increases with increasing angle deviation. The formation of the hcp structure is induced by disordered particles remaining in the center region of the container.

1. Introduction

Recently, colloidal crystals have been studied as materials for photonic devices. Since the radius of colloidal particles is as large as the wavelength of visible light, the colloidal crystals are expected to be used as devices such as optical filters and switches. In particular, a close-packed colloidal crystal with the face-centered cubic (fcc) structure is used as a template for an inverse opal with a three-dimensional full photonic band gap.[1] Many groups have tried to form large grains of close-packed colloidal crystals with the fcc structure. From a theoretical study[2] and an experiment,[3] it was found that the fcc structure is more stable than the hexagonal close-packed (hcp) structure. However, during growth by sedimentation, a mixture of both structures is often formed.[4]

To avoid the formation of the hcp structure, van Blaaderen et al.[5] carried out the sedimentation of colloidal particles on a patterned substrate with a square lattice. When the lattice constant of the square lattice was suitable for the particles, the {100} face of the fcc structure was formed on the substrate. Since the stacking manner on the {100} face of the fcc structure was unique, the formation of the hcp structure was suppressed and, large grains of colloidal crystal with the fcc structure were formed. The sedimentation of colloidal particles on a patterned substrate, which is called colloid epitaxy, is an effective method.[5,6] However, it is necessary to adjust the lattice constant to the particle size precisely to create large grains without defects.

Suzuki et al. [7] succeeded in creating a large colloidal crystal by a simpler method. They carried out the centrifugal sedimentation in a cuboid container. In their experiment, the container was tilted from the centrifugal force, so that solidification started from an edge of the container. The two-dimensional ordering of the colloidal particles occurred along the container walls, and a triangular lattice, which acted as the {111} face of the fcc structure, was formed on the walls. Then, affected by the triangular lattice, the ordering of the particles proceeded in bulk. By controlling the tilted angle, the suitable direction of the growing interface of the solid phase was selected and large grains of the colloidal crystal were formed. In the method, it is not necessary to make a pattern on the container walls, so that we can form large grains of a colloidal crystal without paying attention to the particle radius.

Another simple method, in which we do not need to consider the particle size, is to use an inverted pyramidal-shaped container. Matsuo et al.[8] formed a large colloidal crystal using a large inverted pyramidal pit. Since the apex angle of the pit was suitable, a large colloidal crystal without defects was formed. In the method, the apex angle probably affects the integrity of the colloidal crystal, but it is unclear whether the grain size and structure of the colloidal crystal are sensitive to the angle deviation.

In this paper, keeping the formation of the colloidal crystal in an inverted pyramidal pit in mind, we study the crystallization of Brownian particles in inverted pyramidal containers. We carry out Brownian dynamics simulations with a uniform external force. We focus on the effect of the apex angle of the container on the ordering of the particles.

2. Model and Order Parameters

Our model is the same as that used in our previous studies,[9–14] which is a simple and standard model. The motion of the ith particle is given by

$$\frac{\mathrm{d}\boldsymbol{r}_i}{\mathrm{d}t} = \frac{1}{\zeta}\left(F_{\mathrm{ext}}\mathbf{e}_{\mathrm{ext}} - \sum_{i \neq j} \boldsymbol{\nabla} U(r_{ij}) + \boldsymbol{F}_i^{\mathrm{B}}\right), \tag{1}$$

where ζ is the frictional coefficient and $\boldsymbol{r}_i$ is the position of the ith particle. In the right-hand side, the first term $F_{\mathrm{ext}}\mathbf{e}_{\mathrm{ext}}$ represents a uniform external force, where F_{ext} and $\boldsymbol{e}_{\mathrm{ext}}$ are the force strength and the force direction, respectively. The second term represents the sum of the internal force from the other particles, where $U(r_{ij})$ is the interaction potential between the ith and jth particles. We assume that the interaction potential is a function of the distance between the two particles $r_{ij} = |\boldsymbol{r}_i - \boldsymbol{r}_j|$. In the experiment of Matsuo et $al.$ [8], the interaction potential is considered to be a short one, so that, for simplicity, we use the Weeks–Chandler–Anderson (WCA) potential[15] as the interaction potential. The form of the WCA potential is the same as the repulsive part of the Lennard–Jones potential and given by

$$U(r_{ij}) = \begin{cases} 4\epsilon\left[\left(\dfrac{\sigma}{r_{ij}}\right)^{12} - \left(\dfrac{\sigma}{r_{ij}}\right)^{6} + \dfrac{1}{4}\right] & (r \leq r_{\mathrm{in}}), \\ 0 & (r \geq r_{\mathrm{in}}), \end{cases} \tag{2}$$

where σ is the characteristic length representing the diameter of the particles and $r_{\mathrm{in}} = 2^{1/6}\sigma$. In eq. (1), the third term $\boldsymbol{F}_i^{\mathrm{B}}$ represents an isotropic random force, which satisfies the following relations:

$$\left\langle F_{x,i}^{\mathrm{B}}(t)\right\rangle = \left\langle F_{y,i}^{\mathrm{B}}(t)\right\rangle = \left\langle F_{z,i}^{\mathrm{B}}(t)\right\rangle = 0, \tag{3}$$

$$\left\langle F_{x,i}^{\mathrm{B}}(t)F_{x,i}^{\mathrm{B}}(t')\right\rangle = \left\langle F_{y,i}^{\mathrm{B}}(t)F_{y,i}^{\mathrm{B}}(t')\right\rangle = \left\langle F_{z,i}^{\mathrm{B}}(t)F_{z,i}^{\mathrm{B}}(t')\right\rangle = 2\zeta k_{\mathrm{B}}T\delta_{ij}\delta(t-t'), \tag{4}$$

where $F_{x,i}^{\mathrm{B}}(t)$, $F_{y,i}^{\mathrm{B}}(t)$, and $F_{z,i}^{\mathrm{B}}(t)$ represent the x, y, and z components of the random force. One of the simplest difference equations corresponding to Eq. (1) is given by[16]

$$\tilde{\boldsymbol{r}}_i(\tilde{t} + \Delta\tilde{t}) = \tilde{\boldsymbol{r}}_i(\tilde{t}) + \left(\tilde{F}_{\mathrm{ext}}\mathbf{e}_{\mathrm{ext}} - \sum_{i \neq j} \boldsymbol{\nabla} U(\tilde{r}_{ij})\right)\Delta\tilde{t} + \Delta\tilde{\boldsymbol{r}}_i^{\mathrm{B}}, \tag{5}$$

where the particle positions, time and forces are scaled as $\tilde{\boldsymbol{r}}_i = \boldsymbol{r}_i/\sigma$, $\tilde{t} = t\epsilon/\zeta\sigma^2$, and $\tilde{F}_{\mathrm{ext}} = F_{\mathrm{ext}}\sigma/\epsilon$, respectively. The last term $\Delta\tilde{\boldsymbol{r}}_i^{\mathrm{B}}$, which represents the normalized isotropic displacement by the random force, satisfies the following relations:

$$\left\langle \Delta x_i^{\mathrm{B}}(t)\right\rangle = \left\langle \Delta y_i^{\mathrm{B}}(t)\right\rangle = \left\langle \Delta z_i^{\mathrm{B}}(t)\right\rangle = 0, \tag{6}$$

$$\left\langle \Delta x_i^{\mathrm{B}}(t)\Delta x_i^{\mathrm{B}}(t)\right\rangle = \left\langle \Delta y_i^{\mathrm{B}}(t)\Delta y_i^{\mathrm{B}}(t)\right\rangle = \left\langle \Delta z_i^{\mathrm{B}}(t)\Delta z_i^{\mathrm{B}}(t)\right\rangle = 2\tilde{R}^{\mathrm{B}}\Delta\tilde{t}\delta_{ij}, \tag{7}$$

where $\Delta x_i^{\text{B}}(t)$, $\Delta y_i^{\text{B}}(t)$, and $\Delta z_i^{\text{B}}(t)$ represent the scaled displacement by the random force in the x, y, and z directions during $\Delta \tilde{t}$, respectively, and $\tilde{R}^{\text{B}} = k_{\text{B}}T/\epsilon$.

Since the sedimentation of particles is caused by the external force $\boldsymbol{F}_{\text{ext}}$, the particle density increases and the ordering of the particles starts from the walls. To investigate the ordering of the particles, we introduce three order parameters: d_l, Q_l, and w_l. The order parameter $d_l(i, j)$[17,18] is used to distinguish solidlike particles from liquidlike particles. The definition of $d_l(i, j)$ is given by

$$d_l(i, j) = \sum_{m=-l}^{l} q_{l,m}(i)q_{l,m}^*(j), \tag{8}$$

where

$$q_{l,m}(i) = \frac{1}{n_{\text{n}}} \sum_{j=1}^{n_{\text{n}}} Y_l^m(\theta_{ij}, \phi_{ij}), \tag{9}$$

and $q_{l,m}^*(j)$ is the complex conjugate of $q_{l,m}(j)$. In Eq. (9), n_{n} is the number of neighboring particles and $Y_l^m(\theta_{ij}, \phi_{ij})$ is the spherical harmonics, where the angles θ_{ij} and ϕ_{ij} represent the polar and azimuthal angles, respectively. In the WCA potential,[15] two particles repel each other when the distance between them is smaller than r_{in}. Thus, taking account of the random displacement, we regard the two particles as neighbors if $r_{ij} < 1.1 r_{\text{in}}$. When the ith and jth particles are neighbors and $d_6(i, j) > 0.7$, the connection between the two particles is regraded as a solidlike one. If the ith particle has four or more solidlike connections, the ith particle is considered to be a solidlike particle[18] .

$Q_l(i)$ and $w_l(i)$ are used to determine the local structure of a solidlike particle.[19–23] In our model, the interaction between the particles is short-range repulsion, so that the hcp and fcc structures are expected to be close-packed structures. If $n_{\text{n}} < 10$, the number of neighbors is insufficient for us to determine the local structure precisely. Thus, we estimate $Q_l(i)$ and $w_l(i)$ for the particles that have 10 or more neighbors. The parameters $Q_l(i)$ and $w_l(i)$ are defined as

$$Q_l(i) = \sqrt{\frac{4\pi}{(2l + 1)} \sum_{m=-l}^{l} |q_{l,m}(i)|^2}, \tag{10}$$

$$w_l(i) = \left[\frac{4\pi}{(2l + 1)}\right]^{3/2} \sum_{m_1+m_2+m_3=0} \begin{pmatrix} l & l & l \\ m_1 & m_2 & m_3 \end{pmatrix} \frac{q_{l,m_1}(i)q_{l,m_2}(i)q_{l,m_3}(i)}{Q_l(i)^3}. \tag{11}$$

The integers m_1, m_2, and m_3 change from $-l$ to l while satisfying $m_1 + m_2 + m_3 = 0$. The term in parentheses in Eq. (11) is the Wigner 3-j symbol. In previous studies,[12–14] we regarded the local structure as the fcc structure if $-0.18 < w_4(i) < -0.01$ and $0.175 < Q_4(i) < 0.2$ and as the hcp structure if $0.02 < w_4(i) < 0.15$ and $0.06 < Q_4(i) < 0.15$. We succeeded

in distinguishing the fcc-structured particles from the hcp-structured particles. Thus, in this paper, we also use the same parameter regions to determine the local structures.

3. Results and Discussion

We carry out numerical simulations using the difference equation, Eq. (5). The number of particles N is 22328, the volume fraction is 0.1, $\tilde{R}_b$ is 0.1, the unit time interval $\Delta\tilde{t}$ is 4×10^{-4}, and $\tilde{F}_{ext} = 0.2$.[24] We randomly place particles in a container and move them without an external force to eliminate the effects of the initial particle positions. Then, we add the external force, set the time to be 0, and start simulations.
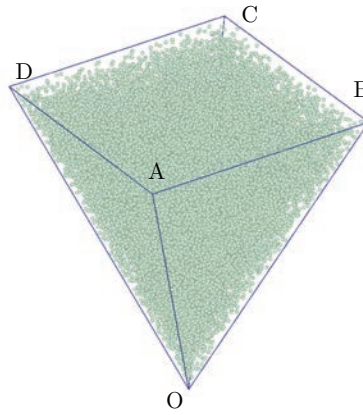
Fig. 1. (color online) Typical shape of container and the position of particles in an early stage $\tilde{t} = 4$. Since $n_{wall} = 1.8$, the angle θ is estimated as $\theta \simeq 68.6°$.

Figure 1 shows a snapshot in an early stage of a simulation. The positive x-and y-directions are parallel to CA and DB, respectively. The positive z-direction is the upward vertical direction. The external force is added to the $-z$ direction, so that solidification starts from around the apex O. The normal directions of the side walls OAB, OBC, OCD, and OAD are $(-1, -1, 1/n_{wall})$, $(1, -1, 1/n_{wall})$, $(1, 1, 1/n_{wall})$, and $(-1, 1, 1/n_{wall})$, respectively, with $n_{wall} = 1.8$. We change n_{wall} while keeping the volume fraction constant, so that the height of the container, L_z, is determined by n_{wall}. We introduce θ, which represents the angle between the normal direction of the side walls and the positive z-direction. The angle θ is related to n_{wall} as $\theta = \tan^{-1}(\sqrt{2}n_{wall})/180°$. The apex angle of the inverted pyramidal container becomes steep with increasing θ. In Fig. 1, the angle θ is estimated as $\theta \simeq 68.6°$

Figure 2 shows snapshots during sedimentation. We cut the container at the plane OBD and view the bulk structure from the positive x-direction. We color the particles to show the difference in the local structures. White (the brightest) particles are dilute liquidlike par-
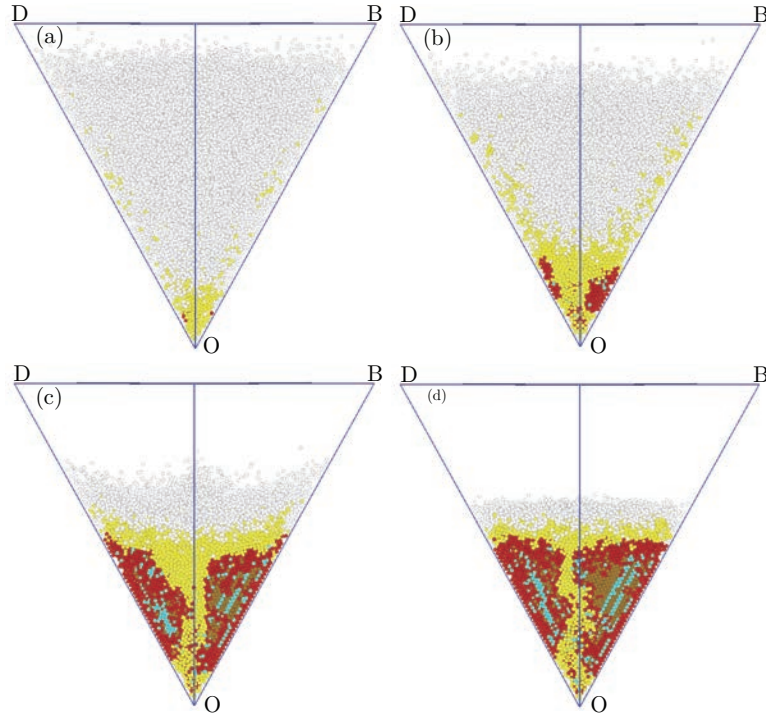
Fig. 2.   (color online) Snapshots in bulk structure at (a) $\tilde{t} = 60$, (b) $\tilde{t} = 100$, (c) $\tilde{t} = 200$, and (d) $\tilde{t} = 400$. Since $n_{\text{wall}} = 1.8$, the angle θ is estimated as $\theta \simeq 68.6°$.

ticles, and yellow (the second brightest) particles are dense liquidlike particles. Blue (the third darkest) particles and brown (the second darkest) particles are particles with the fcc and hcp structures, respectively. Red (the darkest) particles are disordered solidlike particles. In Fig. 2(a), the particle density is high only around the apex O. Then, the high-density region spreads around the side walls and the solidlike particles are formed on the side walls in the bottom region [Fig. 2(b)]. The region with the disordered solidlike particles spreads upward along the side walls. The particles with the fcc and hcp structures are formed parallel to the side walls [Fig. 2(c)]. When solidification finishes, many dense liquidlike particles are left in the center region [Fig. 2(d)]. In our previous study[14] with $n_{\text{wall}} = 1$, the number of the hcp-structured particles, N_{hcp}, was much smaller than that of the fcc-structured particles, N_{fcc}. The hcp-structured particles appeared mainly in the upper side region, and hardly any disordered liquid-like particles remained in the solid. Thus, comparing Fig. 2 and our previous study,[14] we find that the bulk structure is strongly affected by the apex angle.

To investigate the solidification process in more detail, we cut the container in the horizontal direction and show cross sections of Fig. 2(d). In Fig. 3(a), we can see the cross section at $z = 0.38L_z$. The fcc-and hcp-structured particles are parallel to B′C′ and C′D′, which means that the ordered particles preferably form a sheetlike structure along the side walls. In
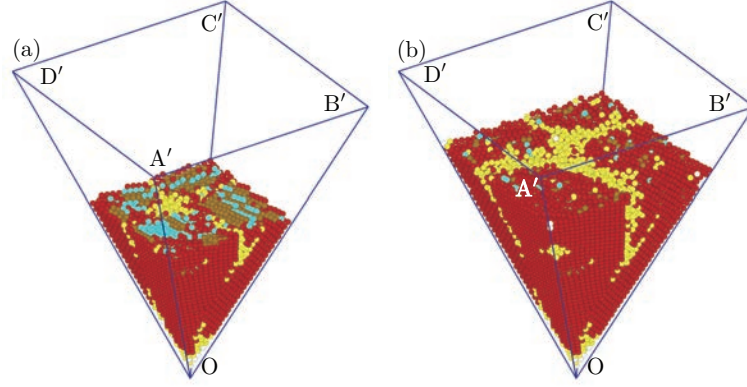
Fig. 3. (color online) Horizontal cross sections at (a) $z = 0.38L_z$ and (b) $z = 0.50L_z$ in a late stage at $\tilde{t} = 400$, in which the sample is the same as that used in Fig. 2(c). OA′ =2OA/3, OB′=2OB/3, OC′ =2OA/3, and OD′=2OD/3. Since $n_{\mathrm{wall}} = 1.8$, the angle θ is given by $\theta \simeq 68.6°$.

Fig. 3(b), we can see the cross section at $z = 0.5L_z$, in which the dense liquidlike particles remain cross-shaped region. From Figs. 2 and 3(b), the solidification process becomes clear. First, the nucleation of the solidlike particles occurs around the edges of the container. The two-dimensional ordering occurs along the walls. Then, affected by the ordering of the particles around the walls, the ordering in bulk proceeds, and the sheetlike structure of the ordered particles is formed. Since the apex angle is not suitable, dense liquidlike particles remain in the region where the grains growing from the four edges OA, OB, OC, and OD coalesce.
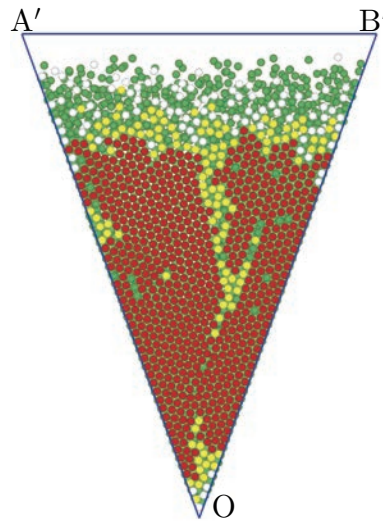

Fig. 4. (color online) Snapshot of the side wall OAB at $\tilde{t} = 400$, in which the sample is the same as that used in Fig. 2(c). OA′ =2 OA/3 and OB′=2OB/3. Since $n_{\mathrm{wall}} = 1.8$, the angle θ is given by $\theta \simeq 68.6°$.

Since the solidification starts from the side walls, we see the two-dimensional structure.

Figure 4 shows a snapshot of the side wall OAB at $\tilde{t} = 400$. We color the particles in the rear side green (the second darkest) to show the particles attaching to the side wall clearly. Since the angle of the apex O is not suitable, the disordered solidlike particles and dense liquidlike particles remain in the center region. The particles trigger off the formation of the hcp structure, and a mixture of the hcp structure and the fcc structure is created. However, almost the entire region is covered with a triangular lattice. The lattice acts as the {111} face of the fcc structure, similarly to in our previous study.[14]
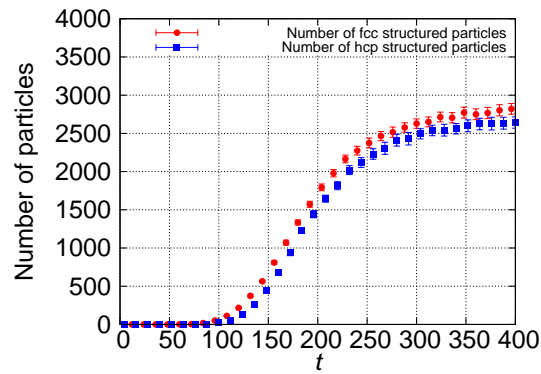

Fig. 5. (color online) Time evolution of the number of the fcc-and hcp-structured particles. $n_{\text{wall}} = 1.8$, so that the angle θ is given by $\theta \simeq 68.6°$. Circles and squares represent the numbers of the fcc-and hcp-structured particles, respectively.

We investigate the structure in the bulk more quantitatively. In Fig. 5, we show the time evolution of the number of the fcc-and hcp-structured particles. N_{fcc} is slightly larger than N_{hcp}. In our previous study,[14] in which the apex angle was suitable, N_{fcc} was much larger than N_{hcp}. Thus, the deviation of the apex angle from the suitable value causes the increase in the number of hcp-structured particles.

We carry out simulations in various containers, and investigate whether the bulk structure is sensitive to the apex angle. Figure 6 shows the dependence of the number of ordered particles on the inclination of the side walls, and Fig. 7 shows snapshots of the bulk structure in three containers. When we neglect the effect of the peak around $\theta = \tan^{-1} \sqrt{2} \simeq 55°$, the number of the ordered particles seems to increase with increasing apex angle, as shown in Fig. 6. When θ is small, the apex is blunt and the pyramidal container is shallow. The particles receive a small pressure from the upper side particles since the width of the settled particles is small. Thus, the solidification does not occur sufficiently. Many liquidlike particles remain and the number of the ordered particles is small [Fig. 7(a)]. On the other hand, the particles
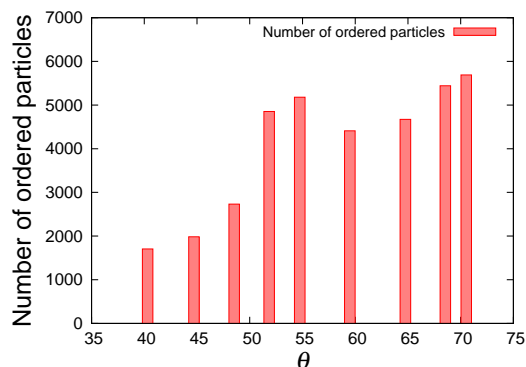
Fig. 6. (color online) Dependence of the number of ordered particles on the inclination of the side walls. The angle θ represents the angle between the normal direction of the side walls and the z-axis.
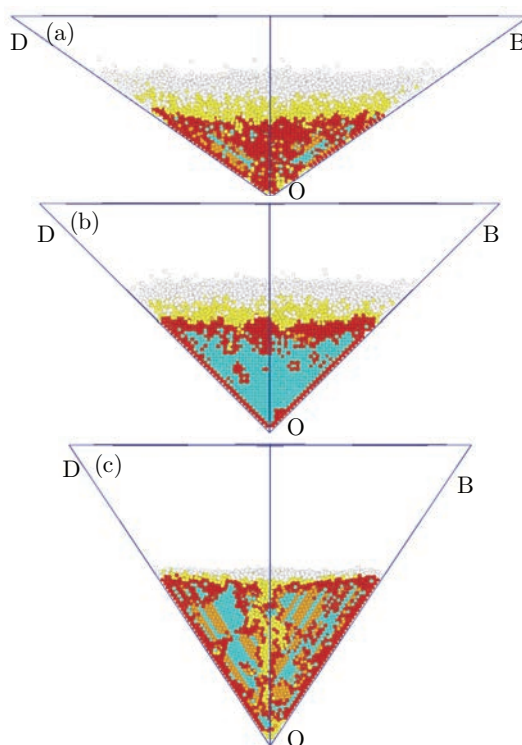
Fig. 7. (color online) Snapshots in bulk structure at $\tilde{t} = 400$ with (a) $n_{\text{wall}}=0.7$ ($\theta \simeq 45°$), (b) $n_{\text{wall}}=1.0$ ($\theta \simeq 55°$), and (c) $n_{\text{wall}}=1.5$ ($\theta \simeq 63°$).

receive a large pressure from the upper side particles with a large θ because the apex angle becomes steep with increasing angle θ, so that a lot of particles are ordered. The number of the ordered particles increases with increasing angle θ, but both the fcc structure and the hcp structure appear [Fig. 7(c)]. When $\theta = \tan^{-1} \sqrt{2}$, the apex angle becomes suitable. The fcc structure can grow in the container without remaining the disordered particles in the center region, so that the number of the ordered solidlike partilces is as high as that with large θ
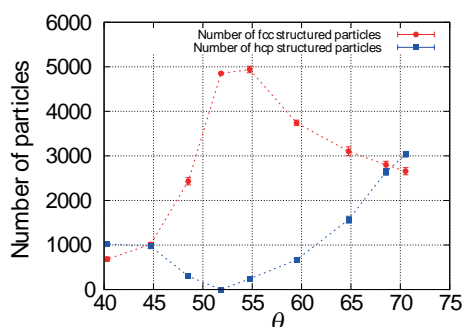
Fig. 7(b)].
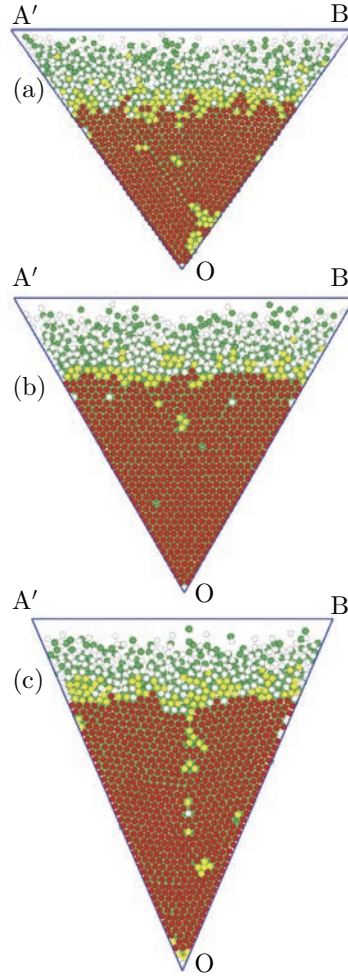
Fig. 8. (color online) Snapshots of the side wall OAB at $\tilde{t} = 400$ with (a) $n_{\text{wall}}=0.7$ ($\theta \simeq 45°$), (b) $n_{\text{wall}}=1.0$ ($\theta \simeq 55°$), and (c) $n_{\text{wall}}=1.5$ ($\theta \simeq 63°$). OA$'$ =2 OA/3 and OB$'$=2OB/3. The samples are the same as those in Fig. 7.

We next describe why the fcc structure grows predominantly with $\theta = \tan^{-1} \sqrt{2}$ when we consider the two-dimensional structure on the side walls. Figure 8 shows snapshots of the side wall OAB in the three cases in Fig. 7. The solidlike particles attaching to the side walls form a triangular lattice in each case. Since a close-packed structure is formed in the bulk affected by the two-dimensional ordering, the fcc structure with the {111} faces on the side walls tends to be formed in the bulk regardless of the apex angle. Thus, the angle θ must be given by $\theta = \tan^{-1} \sqrt{2}°$ to form the fcc structure without forming defects. If θ deviates from $\tan^{-1} \sqrt{2}°$, however, it is geometrically impossible to fill the container with the fcc structure without forming defects. Thus, the disordered particles remain in the bulk and induce the

formation of the hcp structure.

Fig. 9. (color online) Dependence of N_{fcc} and N_{hcp} on the angle θ.

In Fig. 7, almost all the particles in the bulk seem be the fcc structure when $n_{\text{wall}} = 1$ [Fig. 7(b)], but both the hcp structure and the fcc structure are formed in the bulk when $n_{\text{wall}} \neq 1$ [Figs. 7(a) and 7(c)]. Thus, the above explanation of the dependence of the apex angle on the bulk structure seems to agree with the simulation results qualitatively. To confirm the validity of the explanation in more detail, we investigate the dependence of the bulk structure on θ more quantitatively. Figure 9 shows the dependence of N_{fcc} and N_{hcp} on the inclination of the side walls. When $n_{\text{wall}} = 1$, the angle θ is about $55°$ and the container shape is most suitable for the growth of the fcc structure. Almost all the ordered particles are fcc-structured particles around this angle [Fig. 9(a)]. When the angle θ deviates from this angle, the ratio of N_{hcp} to the number of the ordered particles increases with increasing angle deviation. When the deviation of the angle θ from the suitable value is sufficiently large, N_{hcp} becomes as large as N_{fcc} [Fig. 9(b)]. Thus, the results qualitatively agree with our explanation on the dependence of the bulk structure on θ.

4. Conclusion

In this paper, we studied the crystallization of Brownian particles in inverted pyramidal containers by an external force. Changing the apex angle, we investigated how the ordering in bulk is affected by the shape of the pyramidal container. Regardless of the apex angle, solidification first occurs around the edges of the container. Then, the region with the disordered solidlike particles spreads along the wall and two-dimensional ordering on the walls occurs. Affected by the two-dimensional ordering, the ordering of particles proceeds inward. Since a triangular lattice is formed on the side walls regardless of the inclination of the side walls, the fcc structure with the {111} faces on the side walls tends to be formed in the container.

Thus, the inclination of the side walls, with which the fcc structure can be formed without the formation of defects is given by $n_{\text{wall}} = 1$.

If we use a groove as the container, another interface direction is possible as shown in a previous experiment.[8] However, as long as we use a pyramidal container, the disordered particles should remain in the container with unsuitable apex angles due to the geometrical restriction. The disordered particles act as the trigger of formation of many hcp-structured particles, which are rarely seen in the container with a suitable angle. The ratio of N_{hcp} to N_{fcc} increases with increasing deviation of the angle from the suitable angle. N_{hcp} seems to be roughly as large as N_{fcc} with a large deviation of the inclination. Thus, to create a large colloidal crystal with good quality, it is necessary to precisely set the apex angle to a suitable value.

Acknowledgments

References

1) A. Blanco, E. Chomski, S. Grabtchak, M. Ibisate, S. John, S. W. Leonard, C. Lopez, F. Meseguer, H. Miguez, J. P. Mondia, G. A. Ozin, O. Toader, and H. M. Van Diel, Nature **405**, 437 (2000).

2) L. V. Woodcock, Nature **385**, 141 (1997).

3) H. Míguez, F. Meseguer, C. López, A. Mifsud, J. S. Moya, and L. Vázquez, Langmuir **13**, 6009 (1997).

4) J. Zhu, M. Li, R. Rogers, W. Meyer, R. H. Ottewill, STS-73 Space Shuttle Crew, W. B. Russel, and P. M. Chaikin, Nature **387**, 883 (1997).

5) A. V. Blaaderen, R. Ruel, and P. Wiltzius, Nature (London) **385**, 321 (1997).

6) Y. Yin, Z.-Y. Li, and Y. Xia, Langmuir **19**, 622 (2003).

7) Y. Suzuki, A. Mori, M. Sato, and H. Katsuno, J. Cryst. Growth **401**, 905 (2014).

8) S. Matsuo, T. Fujine, K. Fukuda, S. Juodkazis, and H. Misawa, Appl. Phys. Lett. **82**, 4285 (2003).

9) M. Sato, H. Katsuno, and Y. Suzuki, Phys. Rev. E **87**, 032403 (2013).

10) M. Sato, H. Katsuno, and Y. Suzuki, J. Phys. Soc. Jpn. **82**, 084804 (2013).

11) M. Sato, Y. Suzuki, and H. Katsuno, J. Cryst. Growth **401**, 87 (2014).

12) M. Fujine, M. Sato, H. Katsuno, and Y. Suzuki, Phys. Rev. E **89**, 042401 (2014).

13) M. Fujine, M. Sato, T. Toyooka, H. Katsuno, and Y. Suzuki, and T. Sawada, Phys. Rev. E **90**, 032404 (2014).

14) Y. Kanatsu and M. Sato, J. Phys. Soc. Jpn. **84**, 044601 (2015).

15) J. D. Weeks, D. Chandler, and H. C. Anderson, J. Chem. Phys. **54**, 5237 (1971).

16) D. L. Ermak, J. Chem. Phys. **62**, 4189 (1975).

17) P. R. ten Wolde, M. J. Ruiz-Montero, and D. Frenkel, Phys. Rev. Lett **75**, 2714 (1995).

18) M. Marechal, M. Hermes, and M. Dijkstra, J. Chem. Phys. **135**, 034510 (2011).

19) P. J. Steinhardt, D. R. Nelson, and M. Ronchetti, Phys. Rev. B **28**, 784 (1983).

20) M. D. Rintoul and S. Torquato, J. Chem. Phys. **105**, 9258 (1996).

21) W. Lechner and C. Dellago, J. Chem. Phys. **129**, 114707 (2008).

22) A. Panaitescu, K. A. Reddy, and A. Kudrolli, Phys. Rev. Lett. **108**, 108001 (2012).

23) C. Desgranges and J. Delhommelle, Phys. Rev. B **77**, 054201 (2008).

24) As we estimated in our previous study,[14] $\tilde{F}_{\text{ext}}$ is larger than that in a previous experiment.[8] Thus, the ratio of the disordered particles remaining in the bulk may be larger than that in the experiment.[8] When we use a smaller external force, the ratio of the disordered particles in the bulk decreases. However, with a small external force, the pressure that the particles received from the upper particles decreases, so that many liquidlike particles are left in the upper part and the total number of solidlike particles may decrease. Thus, taking account of our previous study,[14] we determine the value of F_{ext}.